

## Scaling and intermittency of brain events as a manifestation of consciousness

P. Paradisi, P. Allegrini, A. Gemignani, M. Laurino, D. Menicucci et al.

Citation: *AIP Conf. Proc.* **1510**, 151 (2013); doi: 10.1063/1.4776519

View online: <http://dx.doi.org/10.1063/1.4776519>

View Table of Contents: <http://proceedings.aip.org/dbt/dbt.jsp?KEY=APCPCS&Volume=1510&Issue=1>

Published by the *AIP Publishing LLC*.

---

### Additional information on AIP Conf. Proc.

Journal Homepage: <http://proceedings.aip.org/>

Journal Information: [http://proceedings.aip.org/about/about\\_the\\_proceedings](http://proceedings.aip.org/about/about_the_proceedings)

Top downloads: [http://proceedings.aip.org/dbt/most\\_downloaded.jsp?KEY=APCPCS](http://proceedings.aip.org/dbt/most_downloaded.jsp?KEY=APCPCS)

Information for Authors: [http://proceedings.aip.org/authors/information\\_for\\_authors](http://proceedings.aip.org/authors/information_for_authors)

### ADVERTISEMENT



**AIP**Advances

*Submit Now*

**Explore AIP's new  
open-access journal**

- **Article-level metrics  
now available**
- **Join the conversation!  
Rate & comment on articles**

# Scaling and intermittency of brain events as a manifestation of consciousness

P. Paradisi\*, P. Allegrini<sup>†,\*\*</sup>, A. Gemignani<sup>‡,\*\*</sup>, M. Laurino<sup>†,\*\*</sup>, D. Menicucci<sup>†,\*\*</sup> and A. Piarulli<sup>§,\*\*</sup>

\**Istituto di Scienza e Tecnologie dell'Informazione (ISTI-CNR), Via Moruzzi 1, 56124 Pisa, Italy.*

<sup>†</sup>*Istituto di Fisiologia Clinica (IFC-CNR), Via Moruzzi 1, 56124 Pisa, Italy.*

\*\**Centro EXTREME, Scuola Superiore Sant'Anna, P.zza Martiri della Libertà 7, 56127 Pisa, Italy.*

<sup>‡</sup>*Dipartimento di Scienze Fisiologiche, Università di Pisa, Via San Zeno 31, 56127 Pisa, Italy.*

<sup>§</sup>*PERCeptual Robotics laboratory (PERCRO), Scuola Superiore Sant'Anna, P.zza Martiri della Libertà 7, 56127 Pisa, Italy.*

**Abstract.** We discuss the critical brain hypothesis and its relationship with intermittent renewal processes displaying power-law decay in the distribution of waiting times between two consecutive renewal events. In particular, studies on complex systems in a “critical” condition show that macroscopic variables, integrating the activities of many individual functional units, undergo fluctuations with an intermittent serial structure characterized by avalanches with inverse-power-law (scale-free) distribution densities of sizes and inter-event times. This condition, which is denoted as “fractal intermittency”, was found in the electroencephalograms of subjects observed during a resting state wake condition. It remained unsolved whether fractal intermittency correlates with the stream of consciousness or with a non-task-driven default mode activity, also present in non-conscious states, like deep sleep. After reviewing a method of scaling analysis of intermittent systems based of event-driven random walks, we show that during deep sleep fractal intermittency breaks down, and re-establishes during REM (Rapid Eye Movement) sleep, with essentially the same anomalous scaling of the pre-sleep wake condition. From the comparison of the pre-sleep wake, deep sleep and REM conditions we argue that the scaling features of intermittent brain events are related to the level of consciousness and, consequently, could be exploited as a possible indicator of consciousness in clinical applications.

**Keywords:** critical brain; fractal intermittency; renewal point processes; diffusion scaling; consciousness.

**PACS:** 05.40.-a, 87.10.-e, 89.75.Da, 87.19.le

## INTRODUCTION

Information processing in the brain is driven by highly nonlinear interactions among neurons, with a high tendency to generate collective behavior, self-organized structures and clustering at several time and space scales. Clusters, or neural assemblies, that emerge at some scale, interact with clusters formed at some other scales with a continuous dynamical interactions among different scales. This is associated with a very rich dynamics that is thought to be associated with the emergence of consciousness [1, 2]. This scale-to-scale interaction in brain dynamics is nowadays recognized to involve universal mechanisms and features of emergent complexity and critical phenomena [3, 4]. Avalanches, scale-free or self-similar behavior, long-range correlations and burstiness are found, both experimentally and theoretically, in many complex systems and, in particular, in neuronal networks [5, 6, 7, 8, 9].

The hypothesis of a critical brain is attracting the interest of the scientific community, with particular attention to the emergence of consciousness. Many neurobiologically plausible models of brain dynamics that are focused on explaining the emergence of consciousness include typical features of critical systems. Among others, it is worth citing the Global Workspace [10, 11], the Dynamic Core [11, 12] and the Operational Architectonics theory [1, 2].

**Criticality in the brain.** The emergence of collective, self-organized behavior, associated with scale-free or power-law behavior and long-range correlations, is typically observed in dynamical systems posed near a *critical point*. In critical phenomena [13] and self-organized criticality [14, 15], the system typically moves towards a critical point, corresponding to a phase transition from an uncorrelated to a correlated condition. This transition is characterized by means of the critical value of a cooperation parameter driving the non-linear coupling among many individual units. The phase-transition hypothesis for the brain dynamics was already discussed by Turing in his pioneering work [16], where he conjectured that an intelligent system cannot “live” neither in a too much correlated condition (order, super-critical), nor in a too chaotic one (disorder, sub-critical). Consequently, brain is expected to operate in the intermediate region between these two extremes, i.e., in a critical condition. This is confirmed by recent neurophysiological literature (see, e.g., [17] or, more recently, [4, 18]). The robust behavior and the great plasticity of the brain dynamics are argued to be strictly related with this critical condition [19].

Many authors investigated the spatial and/or structural complexity of neuronal network models, *in vitro* data and functional Magnetic Resonance Imaging (fMRI) of the human brain and found features in agreement with criticality. In particular, the authors of Refs. [5, 6, 7] found a scale-free distribution of avalanche (or cluster) sizes, which is a signature of spatial and structural long-range correlations, in network models and *in vitro* data. The authors of Refs. [3, 4] studied the functional connectivity of the brain defined through the network of above-threshold cross-correlations derived from fMRI data, which is again a structural property. They evaluated the degree distribution, being the degree of a node the number of links of that node with other nodes, and found a scale-free degree distribution similar to that of the Ising magnetization model at the critical point, corresponding to a second-order phase transition in the magnetization field.

**Intermittency in critical systems.** The above cited studies about criticality in the brain are focused on the spatial or structural complexity. A often overlooked property is the temporal complexity, where the focus is on the *time* long-range correlations with power-law decay (equivalent to  $1/f$  noise) and on *time intermittency*, which is defined by the presence of *crucial events* in the complex/critical system.

The authors of Refs. [8, 20, 21] found that the fluctuations of a random field at the critical point, i.e., the “order parameter” averaging microscopic fluctuations, are described in terms of a *Type-I intermittent* dynamical map similar to the well-known Manneville map [22], which mimics turbulent bursting. This kind of dynamical systems is characterized by the presence of a marginally unstable point determining an alternation between long time intervals with calm motion and short-time bursting events. These events, occurring in the temporal evolution of the order parameter, are described by a serial fractal

point process, i.e., a sequence of intermittent events that: (a) occur randomly in time and (b) display a slow (power-law) decay in the distribution of inter-event or Waiting Times (WTs). Notice that this point process has to be interpreted as a birth-death process of cooperation, where the cooperation is here represented by the intermittent formation and decay of neural assemblies in the brain dynamics. Type-I intermittency is in agreement with a fast decay of memory in correspondence of event occurrences. In the language of stochastic processes, this is described by a *renewal point process* [23], which is defined by the condition of mutual statistical independence of the events and, consequently, of the WTs. In other words, the macroscopic fluctuations of a critical system are driven by a renewal point process, which is the mathematical tool used here to describe intermittency and, in the case of a self-similar or fractal distribution of WTs, *fractal intermittency*. The renewal condition is related to burstiness with fast memory decay and it was found to characterize the intermittency features of several complex systems, from blinking quantum dots [24, 25] to turbulence [26, 27, 28] and brain dynamics [9]. The renewal property seems to play a crucial role in the perturbation of complex systems [29, 30, 31, 32, 33] and it is a fundamental assumption in the derivation of a new Fluctuation-Dissipation Theorem (FDT) based on renewal events [34, 35], whose main prediction is that two complex systems have a maximum interaction when they have similar complexities. The power-law relaxation foreseen by this new FDT was also experimentally validated in the weak turbulence regime of a liquid crystal [36]. Regarding biological systems and, in particular, brain dynamics, we can roughly say that the renewal condition allows to reduce the disorder of the system, as the entropy is significantly increased only in correspondence of event occurrences, while a long memory characterizes the system's evolution in between two events, being this related to the observed long-range correlations. At the same time, the dynamics of events, associated with metastable states, allows for a greater capability of adaptation to external stimuli [2]. Thus, the renewal condition seems to be the only one that can deal, at the same time, with the need of a slow disorder increase (long-range correlations) and a sufficiently rapid adaptability to environmental stimuli (memory erasing events).

**Intermittency and consciousness.** The existence of crucial events in the brain is well-established, as spontaneous neuronal activity exhibits relatively quiet periods in alternation with chaotic or bursty periods. Such brain events can be extracted from ElectroEncephaloGram (EEG) data with detection algorithms. Events are here defined as abrupt transitions or Rapid Transition Processes (RTPs) [1, 37, 38]) to and from metastable states, via multichannel EEGs [9]. On short time scales brain events typically display a complex structure in terms of neuronal avalanches [39].

Exploiting the concept of RTP events, we investigated the temporal complexity of brain dynamics in terms of intermittency features [9, 39]. We found that a serial renewal process of global integration exists in the human brain during a *resting state* wake condition and that this renewal process has well-defined scaling exponents in both distributions of avalanche sizes and inter-event times [9, 39]. These scaling exponents, being a signature of Type-I fractal intermittency, confirm the critical brain hypothesis [19]. The scaling exponents were evaluated through the diffusion scaling of different random walks driven by the RTP events (see details in the next section). This approach based on diffusion scaling allowed to get a robust estimation of the intermittency exponent or

*complexity index*  $\mu$ , i.e., the exponent of the inverse power-law tail in the WT distribution:  $\psi(\tau) \sim 1/\tau^\mu$ . It is worth noting that similar approaches, based on brain events and point processes, have been recently applied, confirming the robust and universal critical behavior of brain dynamics and neuronal networks [40, 41].

All the above findings lead to the idea that consciousness is related with the emergence of criticality and fractal intermittency. However, this is just a hypothesis as it is not yet clear if this renewal fractal process is uniquely associated with consciousness or with a non-task-driven default mode activity [42], also present in non-conscious states like deep sleep.

In this paper we clarify this point by evaluating the event-driven diffusion scaling of EEG data collected from the observation of healthy human subjects during sleep. The statistical analysis we use is essentially the same as in Ref. [9]. In “Data Description and Methods of Analysis” section we describe the dataset and the methods of data analysis. In particular, we will introduce the diffusion scaling method. In “Results and Discussion” section we show our results and we discuss the hypothesis that the emergence of intermittent events described by a (serial) renewal fractal process and of anomalous diffusion is a signature of consciousness, while the lack of fractal features and the emergence of normal diffusion could characterize non-conscious states.

## DATA DESCRIPTION AND METHODS OF ANALYSIS

A normal night’s sleep consists of a few (from 4 to 6) cycles, each cycle consisting of different phases, defined on the presence of different “waves”, or graphoelements, and specific rhythms. After a pre-sleep wakefulness, the first cycle begins with a shallow sleep called N1. As the sleep deepens, due to the diminished presence of various neurotransmitters, sleep phases N2 and N3 (or Slow Wave Sleep, SWS) are visited one or more times, till the Rapid Eye Movement (REM) phase (typically a dreaming phase) occurs, that marks the end of the cycle. The phases N1, N2 and N3 (or SWS) are globally referred to as Non-REM (NREM) phase. At variance with NREM phase, REM is characterized by a high level of the acetylcholine (AC) neurotransmitter. At the end of the first cycle, a second cycle begins, with or without N1 or wakefulness episodes (Wakefulness After Sleep Onset, WASO), with the presence of NREM sleep (AC again drops to low values), again ending with a REM phases, and so on.

**Data set.** Our data set is composed of 29 whole-night high-density (128 channel, 4ms sampling time) EEG recordings. Subjects slept two nights with the same experimental setup, namely after an adaptation night the second one was recorded. All subjects signed informed consent according to local ethical committees. Through visual inspection of the polygraphic traces, namely a selection of few EEG channel plus miogram (muscle tone intensity) and oculogram (eye movements) all recordings were segmented into different cycles and phases. For the purpose of the present paper, however, we will focus on global properties of sleep in the various phases and we will freely make recourse to grand averages over the 29 whole-night recordings. Artifacts were semiautomatically removed, and only artifact-free segments of time duration longer than 3 min-

utes were kept for the RTP detection. We use only segments of the first cycle, as signal quality decreased in subsequent cycles.

**Rapid Transition Processes.** Herein, for each EEG channel, pass-band filtered between 0.3 and 40 Hz (Chebyshev II filter algorithm), RTPs are extracted as a “significant” selection of intersection between two different moving averages of the Hilbert transform of the signal modulus. Moving averages have windows of 5 and 125 ms, respectively. By significant we mean that we select only the points where the intersection between the two curves is above a threshold angle. To do this we select a 125 ms window surrounding the intersection and compute the sum of the modulus of the difference between the two curves. For each channel significant RTPs are those in the highest decile (the ones higher than 90% are chosen). This method is inspired and similar to that introduced in Ref. [37], but with slightly differences. We however proved in [43] that our subsequent analysis is robust with respect to a variation of event definition.

We are here interested on global events, i.e., on the “simultaneous” occurrences of RTP in different EEG channels. For each EEG recording, the sequence of coincidences, or (concurrent) Multi-Channel RTPs (MC-RTPs), is obtained from single-channel RTPs via the introduction of two thresholds: The first one,  $\Delta t_c$ , defines the maximum time distance for two single-channel RTPs (from different channels) to be considered concurrent; the second one,  $N_t$ , defines the minimum number of concurrent single-channel RTPs required for a MC-RTPs to be recorded as a global event. Since events that have a distance less than  $\Delta t_c$  are considered to be simultaneous,  $\Delta t_c$  must be small. We herein use  $\Delta t_c = 4$  ms, equal to the instrumental sampling time, and  $N_t = 5$ .

**Event-driven random walks and diffusion scaling.** The random walks driven by renewal events [9, 28] are inspired to the Continuous Time Random Walk (CTRW) of Montroll and co-workers [44, 45]. In CTRW it is allowed to have random time steps, corresponding to a sequence of WT from a renewal process. Here, the WT sequences derived from the EEG recordings are used to define two different CTRWs driven by the same RTP global events. Firstly, we introduce a discrete artificial signal  $\xi(t)$ , i.e., a kind of random discontinuous velocity that changes value only in correspondence of event occurrences. In Figs. 1 and 2 a sketch of the two signals  $\xi(t)$  is reported. The times  $t_0, t_1, t_2, \dots$  correspond to the occurrence of the events 0, 1, 2, ..., while  $\tau_1, \tau_2, \dots$  are the WTs, i.e., the time interval between the events 0 and 1, the events 1 and 2 and so on. In particular, we have:

- (a) Asymmetric Jump (AJ) rule:  
the walker makes a positive jump ( $\xi(t_n) = 1$ ) in correspondence of each event  $n$ , otherwise it stands ( $\xi(t) = 0$ ). Then,  $\xi(t)$  is a sequence of pulses of constant intensity.
- (b) Symmetric Jump (SJ) rule:  
as in the AJ rule, but the walker can make positive or negative jumps in correspondence of an event:  $\xi(t_n) = \pm 1$ . The sign  $\pm$  is chosen with a coin tossing prescription.

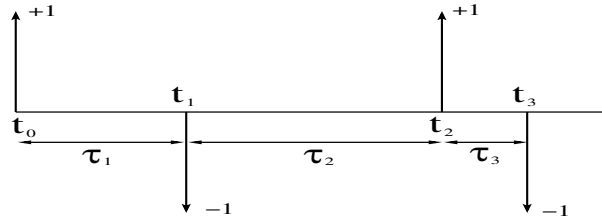


**FIGURE 1.** The SJ walking rules for the “velocity signal”  $\xi(t)$ .

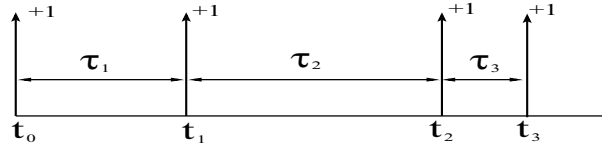


**FIGURE 2.** The AJ walking rules for the “velocity signal”  $\xi(t)$ .

Then, from the artificial signal  $\xi(t)$  the diffusion variable of the CTRW is defined as follows:

$$X(t) = X_0 + \sum_{j=0}^{j=t} \xi(j) \Delta t, \quad (1)$$

being  $\Delta t$  the sampling time of the experimental time series.

The scaling properties of these random walks were extensively investigated in several papers (see [9, 27, 28] for a brief review) by applying the analytical methods of CTRW. Here we are interested in the scaling exponent  $H$  of the second moment

$$\sigma^2(t) = \langle (X(t) - \bar{X})^2 \rangle \sim t^{2H}, \quad (2)$$

where  $\bar{X}$  is the mean value of  $X(t)$ .

Analytical expressions of the scaling  $H$  as a function of the complexity index  $\mu$  were determined in the case of renewal WTs with inverse power-law tail:  $\psi(\tau) \sim 1/\tau^\mu$ . These

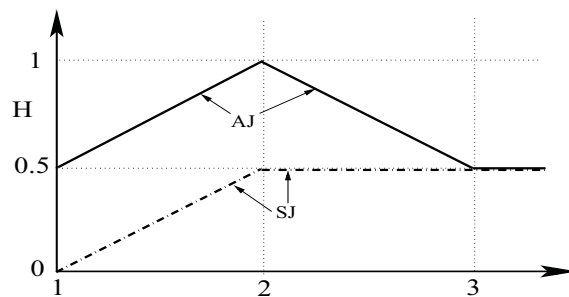


**FIGURE 3.** Diffusion scaling  $H$  vs. complexity index  $\mu$  for SJ and AJ walking rules: AJ (continuous line), SJ (dotted-dashed line).

expressions  $H = H(\mu)$  are reported in Fig. 3 and summarized in the following:

(AJ)

$$H_{AJ} = \begin{cases} \mu/2; & 1 < \mu < 2 \\ 2 - \mu/2; & 2 \leq \mu < 3 \\ 1/2; & \mu \geq 3 \end{cases} \quad (3)$$

(SJ)

$$H_{SJ} = \begin{cases} (\mu - 1)/2; & 1 < \mu < 2 \\ 1/2; & \mu \geq 2 \end{cases} \quad (4)$$

Both rules give a normal scaling  $H = 1/2$  for  $\mu \geq 3$ , corresponding to normal (Gaussian) diffusion. For the SJ rule this is true also in the range  $2 < \mu \leq 3$ , while AJ rule is super-diffusive ( $H > 1/2$ ) in all the interval  $1 < \mu < 3$ . On the contrary, the SJ rule is sub-diffusive ( $H < 1/2$ ) for  $1 < \mu < 2$ . We note that, if the WTs comes from a Poisson process, the value of  $H$  is again  $1/2$  and, in the long-time, we have a Gaussian diffusion.

The joint use of these walking rules can be used to evaluate the value of the  $\mu$  by inverting the expressions given in Eqs. (3-4). It can be seen from Fig. 3 that  $H_{AJ}(\mu)$  is not an invertible function, as the same value of  $H$  corresponds to two distinct values of  $\mu$ , one smaller and the other greater than 2. When  $H_{SJ} < 1/2$  it results  $\mu < 2$  and both rules, i.e., the associated values of  $\mu$  derived from AJ and SJ rules, could be compared to each other. On the contrary, for  $H_{SJ} = 1/2$ , a value of  $\mu$  cannot be derived from the SJ rule, but we can assume  $\mu > 2$ . For this reason, the SJ rule could be used to discriminate between  $\mu < 2$  and  $\mu > 2$ , overcoming the ambiguity of AJ rule.

**Detrended Fluctuation Analysis.** The diffusion scaling  $H$  of the two random walks introduced above is estimated by means of Detrended Fluctuation Analysis (DFA) [46]. We briefly recall the main steps of this method:

- For a discrete time  $L = 4, 5, \dots$ , the time series of the diffusion process  $X(t)$  is split into not-overlapping time windows of length  $L$ :  $[kL + 1, kL + L]$ . The window number is given by  $[M/L]$ , i.e., the integer part of  $M/L$ , being  $M$  the total length of the time series.
- For each time window  $[kL + 1, kL + L]$  ( $k = 0, 1, \dots, [M/L]$ ), the local trend is evaluated with a least-squares straight line fit:  $\bar{X}_{k,L}(t) = a_{k,L}t + b_{k,L}$ ;  $kL < t \leq (k + 1)L$ .
- The fluctuation is derived in the usual way:  $\tilde{X}_{k,L}(t) = X(t) - \bar{X}_{k,L}(t) = X(t) - a_{k,L}t - b_{k,L}$ ;  $kL < t \leq (k + 1)L$ .
- For a given time scale  $L$ , the mean-square deviation of the fluctuation is calculated over every window:

$$F^2(k, L) = \frac{1}{L} \sum_{t=kL+1}^{(k+1)L} \tilde{X}_{k,L}^2(t) = \frac{1}{L} \sum_{t=kL+1}^{(k+1)L} (X(t) - \bar{X}_{k,L}(t))^2 \quad (5)$$

- Finally, an average over the windows is performed:

$$F^2(L) = \frac{1}{[M/L]} \sum_{k=0}^{[M/L]} F^2(k, L) \quad (6)$$

In the case of a self-similar process, it results:  $F(L) \sim L^H$ . Then, by defining  $z = \log(F(L))$  and  $y = \log(L)$ , it is possible to apply a least-squares straight line fit:

$$z = Hy + C, \quad (7)$$

where  $C$  is a constant.

**Improvement of statistical accuracy in DFA.** Given a time series of total length  $L$ , the DFA evaluation is reliable up to about  $L/10$  and this is due to the lack of statistics in the long-time regime. However, we do not have only one time series, but several independent time segments, each one separated from the others by at least one artifact or phase shift in the original EEG recording. Several DFA curves can be obtained, one for each time segment, and then averaged to get a mean DFA curve. In this way, we are able to compute DFA up to a time given by the maximum among the values  $L_i/10$ , that is  $\max_i(L_i/10)$ , where  $i$  runs over all time segments and  $L_i$  is the total duration time of the  $i$ -th time segment. Actually, the statistical accuracy remains stable up to a time given by  $\min_i(L_i/10)$  and then decreases for longer time scales. In fact, the number of segments entering the average decreases very rapidly when approaching the time scale  $\max_i(L_i/10)$ .

We improved the statistical accuracy on longer time scales, without the risk of making the running window explore segments that belong to different segments. Firstly, for each sleep phase, we evaluated the minimal duration time:  $L_m = \min_i(L_i)$ ; then, for each segment, we computed the DFA up to time  $L_m$ ; finally, we performed the average over all the segments. Note that  $L_m$  is not only 10 times greater than  $\min_i(L_i/10)$ , but it is also greater than  $\max_i(L_i/10)$ . With this approach, a much better accuracy on long time scales is obtained. In fact, even if the statistical accuracy is low for the segments with the shortest duration times, the number of segments entering the average is greatly increased in the time range between  $\min_i(L_i/10)$  and  $L_m = \min_i(L_i)$ , as all segments always enter in the average operation.

## RESULTS AND DISCUSSION

Criticality has been found both in neuronal networks (models and *in vitro*, see Refs. [5, 6, 7]) and human brain [3, 4] by investigating the spatial and structural complexity, while temporal complexity, i.e., time intermittency, in brain EEG was investigated in our previous papers (see Refs. [9, 39]). In particular, from the analysis of EEG data in resting state (wakefulness) condition we found that the brain (RTP) events introduced by the authors of Refs. [1, 37] are driven by an underlying renewal fractal point process with well-defined scaling properties (**fractal intermittency**). As already said in “Introduction” section, it is not clear if fractal intermittency is uniquely associated with

consciousness or with a non-task-driven default mode activity [42], also present in non-conscious states like deep (NREM) sleep. To clarify this point, let us summarize some observations about consciousness:

1. the conscious brain is associated with an emerging “giant cluster” or Global Workspace [10]) that co-exist with clusters of any size having scale-free size distribution, in analogy with what happens in critical systems [6, 7];
2. Conscious scenes are unitary and occur serially: only one scene at a time takes place [10];
3. consciousness is a sequence of metastable states (giant clusters), which reflect rapidly adaptive selection mechanisms in perception and memory; in the consciousness theory of Baars [10], the Global Workspace is an emerging serial process that, in some way, selects only one scene at a time from an underlying set of parallel scenes, and only this selected scene comes into consciousness;
4. In conscious states, there’s a competition among cooperative global integration and autonomous fragmentation; the interplay of these two components constitutes the metastable regime of brain dynamics and determines the complex intermittent behavior in the EEG field [2, 12, 47].
5. the renewal fractal process derived from EEG data, which is defined by the sequence of renewal RTP events, is a particular serial process, as only a global metastable state (giant cluster) at a time takes place and the short-time RTP events mark the death of a metastable state and the birth of a new one [9, 39].

From the above observations, we are then lead to make the following assumption:

The **renewal point process** describing **fractal intermittency**, which is experimentally defined in EEG data by the sequence of **global RTP events** with inverse power-law distributed WTs, is a **correlate of consciousness**.

We validate this assumption by comparing different states of consciousness in healthy subjects during sleep. In “Data Description and Methods of Analysis” section we have already given a description of the dataset and of the methods used to analyze the EEG data, which can be summarized as follows: (a) segmentation and artifact removal; (b) RTP detection, global brain events (c) computation of event-driven random walks (SJ and AJ) and estimation of second moment scaling  $H$  by applying DFA. The diffusion scaling  $H$  of the SJ rule is definitively  $H = 0.5$  for all time segments and subjects and, then, also for the mean DFA. This is a signature that the complexity index  $\mu$  is greater than 2. In Fig. 4 we show the square root of the second moment  $\sigma(t)$  for the AJ rule, averaged over all subjects and nights and over the time segments of sleep cycle I as explained at the end of “Data description and Methods of Analysis” section. The second moment scaling  $H$  switches from an anomalous diffusion scaling ( $H = 0.75$ ) in the case of (pre-sleep) wake and REM phases to a normal diffusion scaling ( $H = 0.5$ ) in deep (SWS) sleep. Inverting Eq. 3, this means that in wake and REM phases, which are conscious states, we get an average value  $\mu = 2.5$ , thus giving fractal intermittency and long-range correlations, whereas in the deep (SWS) sleep phase we get  $\mu > 3$ . We recall that normal diffusion ( $H = 0.5$ ) is also in agreement with a Poisson condition, i.e., with exponentially distributed WTs or, more realistically, with an exponential cut-off emerging at relatively short WTs and, thus, with short-time correlations.

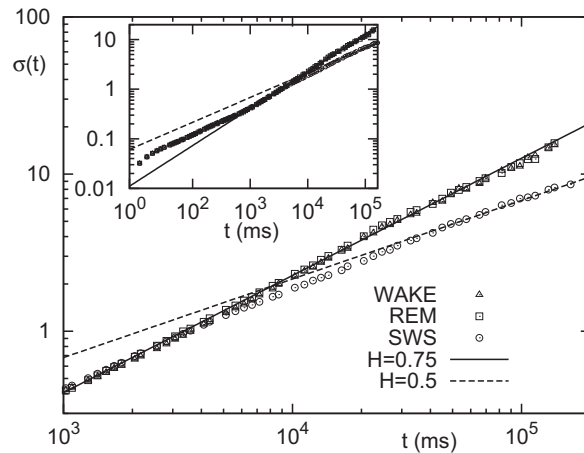


**FIGURE 4.** Asymptotic time range in the DFA computed for AJ rule applied to different sleep phases (cycle I). Continuous and dashed lines are a guide to the eye for the slopes  $H = 0.75$  and  $H = 0.5$ , respectively. In the inset we report the entire time range over which the DFA has been computed. Notice that, in the short-time range, the DFA of the three phases (WAKE, REM and SWS) are essentially superposed, all displaying normal diffusion.

The normal diffusion regime during SWS phase could be explained in terms of the fragmentation of the Global Workspace into local, independent, functional units working in parallel, which is a condition known to be associated with the lack of consciousness. Notice that the fragmentation is related to the large number of Sleep Slow Oscillations (SSOs) during SWS [48], which determine a reset of the neuronal activity by means of a hyper-polarizing wave putting most neurons in a down-state, i.e., a state far from the activation threshold of the membrane potential. This is also called “electrical silence”. Finally, from a purely descriptive point of view, we can conclude that the result of Fig. 4 demonstrates that the scaling  $H$ , and the associated complexity index  $\mu$ , could be proposed as a reliable indicator of conscious states. The interpretation of these results deserve further investigations that, however, will be the focus of future research work.

## REFERENCES

1. A. A. Fingelkurts, and A. A. Fingelkurts, *Brain and Mind* **2**, 261–296 (2001).
2. A. A. Fingelkurts, A. A. Fingelkurts, and C. F. H. Neves, *Phys. Life Rev.* **7**, 195–249 (2010).
3. D. Fraiman, P. Balenzuela, J. Foss, and D. R. Chialvo, *Phys. Rev. E* **79**, 061922 (2009).
4. D. R. Chialvo, *Nature Phys.* **6**, 744–750 (2010).
5. J. M. Beggs, and D. Plenz, *J. Neurosci.* **23**, 11167–11177 (2003).
6. D. Plenz, and T. C. Thiagarjan, *Trends Neurosci.* **30**, 101–110 (2007).
7. G. L. Pellegrini, L. de Arcangelis, H. J. Hermann, and C. Perrone-Capano, *Phys. Rev. E* **76**, 016107 (2007).
8. M. Turalska, B. J. West, and P. Grigolini, *Phys. Rev. E*, **83**, 061142 (2011).
9. P. Allegrini, D. Menicucci, R. Bedini, L. Fronzoni, A. Gemignani, P. Grigolini, B.J. West, and P. Paradisi, *Phys. Rev. E* **80**, 061914 (2009).
10. B. J. Baars, *A cognitive theory of consciousness*, Cambridge University Press, Cambridge, UK, 1998.
11. G. M. Edelman, J. A. Gally, and B. J. Baars, *Front. Psychol.* **2**, 4 (2011).

12. G. Tononi, and G.M. Edelman, *Science* **282**, 1846–1851 (1998).
13. D. Sornette, *Critical phenomena in natural sciences*, Springer-Verlag, Berlin, 2006.
14. H. J. Jensen, *Self-organized criticality*, Cambridge University Press, Cambridge, 1998.
15. P. Bak, C. Tang, and K. Wiesenfeld, *Phys. Rev. Lett.* **59**, 381 (1987); P. Bak, C. Tang and K. Wiesenfeld, *J. Phys. A* **38**, 364 (1988).
16. A. M. Turing, *Mind* **59**, 433–460 (1950).
17. D. R. Chialvo, and P. Bak: *Neuroscience* **90**, 1137–1148 (1999).
18. G. Werner, *Biosystems* **96**, 114–119 (2009).
19. E. Tagliazucchi, and D. R. Chialvo, arXiv: 1103.2070v1 [q-bio.NC] (2011).
20. Y. F. Contoyiannis, and F. K. Diakonou, *Phys. Lett. A* **268**, 286–292 (2000).
21. Y. F. Contoyiannis, F. K. Diakonou, and A. Malakis *Phys. Rev. Lett.* **89**(3), 035701 (2002).
22. P. Manneville: *J. Physique (France)* **41**(11), 1235–1243, (1980).
23. D. R. Cox, *Renewal Theory*, Methuen, London, 1962.
24. P. Paradisi, P. Allegrini, F. Barbi, S. Bianco, and P. Grigolini, *AIP Conf. Proc.* **800**(1), 92–97, 2005.
25. S. Bianco, P. Grigolini, and P. Paradisi, *J. Chem. Phys.* **123**(17), 174704, 2005.
26. P. Paradisi, R. Cesari, D. Contini, A. Donateo, and L. Palatella, *Eur. Phys. J. Special Topics* **174**, 207–218, (2009).
27. P. Paradisi, R. Cesari, A. Donateo, D. Contini, and P. Allegrini, *Nonl. Proc. Geoph.* **19**, 113–126 (2012).
28. P. Paradisi, R. Cesari, A. Donateo, D. Contini, and P. Allegrini, *Rep. Math. Phys.* **70**, 205–220 (2012).
29. O. C. Akin, P. Paradisi, and P. Grigolini, *Physica A* **371**(2), 157–170 (2006).
30. P. Allegrini, F. Barbi, P. Grigolini, and P. Paradisi, *Chaos, Solit. & Fract.* **34**(1), 11–18 (2007).
31. S. Bianco, P. Grigolini, and P. Paradisi, *Chem. Phys. Lett.* **438** (4-6), 336–340 (2007).
32. P. Paradisi, R. Cesari, and P. Grigolini, *Cent. Eur. J. Phys.* **7**(3), 421–431 (2009).
33. O. C. Akin, P. Paradisi, and P. Grigolini, *J. Stat. Mech.: Theory Exp.*, P01013, (2009).
34. P. Allegrini, M. Bologna, P. Grigolini, and B. J. West, *Phys. Rev. Lett.* **99**(1), 010603 (2007).
35. P. Allegrini, P. Paradisi, D. Menicucci, R. Bedini, A. Gemignani, and L. Fronzoni, *J. Phys.: Conf. Series* **306**, 012027 (2011).
36. L. Silvestri, L. Fronzoni, P. Grigolini, and P. Allegrini, *Phys. Rev. Lett.* **102**, 014502 (2009).
37. A. Y. Kaplan, A. A. Fingelkurts, A. A. Fingelkurts, B. S. Borisov, and B. S. Darkhovskiy, *Signal Process.* **85**, 2190–2212 (2005).
38. A. A. Fingelkurts, and A. A. Fingelkurts, *Open Neuroimag. J.* **2**, 73–93 (2008).
39. P. Allegrini, P. Paradisi, D. Menicucci, and A. Gemignani, *Front. Physiol.* **1**, 128 (2010).
40. F. Lombardi, H. J. Herrmann, C. Perrone-Capano, D. Plenz, and L. de Arcangelis, *Phys. Rev. Lett.* **108**, 228703 (2012).
41. E. Tagliazucchi, P. Balenzuela, D. Fraiman, and D. R. Chialvo, *Front. Physiol.* **3**, 15 (2012).
42. M. E. Raichle, A. M. MacLeod, A. Z. Snyder, W. J. Powers, D. A. Gusnard, and G. L. Shulman, *Proc. Natl. Acad. Sci. USA* **98**, 676–682 (2001).
43. P. Allegrini, D. Menicucci, R. Bedini, A. Gemignani, and P. Paradisi, *Phys. Rev. E* **82**, 015103 (2010).
44. E. W. Montroll, *Proc. Symp. Appl. Math., Am. Math. Soc.* **16**, 193–220 (1964).
45. G. H. Weiss, and R. J. Rubin, *Adv. Chem. Phys.* **52**, 363–505, 1983.
46. C.-K. Peng, S. V. Buldyrev, S. Havlin, M. Simons, H. E. Stanley, and A. L. Goldberger, *Phys. Rev. E* **49**, 1685 (1994).
47. G. Tononi, *Biol. Bull.* **215**, 216–242 (2008);
48. D. Menicucci, A. Piarulli, U. Debarnot, P. d’Ascanio, A. Landi, and A. Gemignani, *PLoS One* **4**, e7601 (2009).